

The detection of ruthenium chloride clusters by laser desorption ionization-mass spectrometry of $\text{RuCl}_3 \cdot 3\text{H}_2\text{O}$

Alexander G. Boncheff and Mario A. Monteiro

Abstract: The production of gas-phase singly charged ruthenium chloride anionic complexes by laser desorption ionization of $\text{RuCl}_3 \cdot 3\text{H}_2\text{O}$ is reported. The $[\text{Ru}_x\text{Cl}_y]^-$ clusters could only be detected in the absence of the matrix component in the negative mode. The cluster compositions observed were $[\text{RuCl}_4]^-$, $[\text{RuCl}_5]^-$, $[\text{Ru}_2\text{Cl}_6]^-$, $[\text{Ru}_2\text{Cl}_7]^-$, $[\text{Ru}_3\text{Cl}_9]^-$, $[\text{Ru}_4\text{Cl}_{11}]^-$, and $[\text{Ru}_5\text{Cl}_{12}]^-$. With the aid of density functional theory calculations, we proposed feasible structures for each ruthenium chloride cluster, in which Ru–Ru bonds and Cl bridges were a common characteristic.

Key words: ruthenium, laser desorption ionization, metal clusters, $\text{RuCl}_3 \cdot 3\text{H}_2\text{O}$, density functional theory, mass spectrometry.

Résumé : Faisant appel à la technique d'ionisation par désorption au laser du $\text{RuCl}_3 \cdot 3\text{H}_2\text{O}$, on a réalisé la production en phase gazeuse de complexes anioniques du chlorure de ruthénium portant une seule charge. Dans le mode négatif, on ne peut détecter la présence des agrégats de $[\text{Ru}_x\text{Cl}_y]^-$ qu'en l'absence de la composante matricielle. On a pu observer les cations de composition $[\text{RuCl}_4]^-$, $[\text{RuCl}_5]^-$, $[\text{Ru}_2\text{Cl}_6]^-$, $[\text{Ru}_2\text{Cl}_7]^-$, $[\text{Ru}_3\text{Cl}_9]^-$, $[\text{Ru}_4\text{Cl}_{11}]^-$ et $[\text{Ru}_5\text{Cl}_{12}]^-$. En se basant sur des calculs selon la théorie de la fonctionnelle de la densité, on propose des structures plausibles pour chacun des agrégats de chlorure de ruthénium dans lesquels des liaisons Ru–Ru et des ponts Cl sont des caractéristiques communes.

Mots-clés : ruthénium, ionisation par désorption au laser, agrégats métalliques, $\text{RuCl}_3 \cdot 3\text{H}_2\text{O}$, théorie de la fonctionnelle de la densité, spectrométrie de masse.

[Traduit par la Rédaction]

Introduction

Part of our research program focuses on the development of new methods for the structural characterization of complex bacterial polysaccharides (PSs). We envisaged that the coupling of ruthenium to PSs, especially those expressing amine moieties, may help us obtain less convoluted NMR spectra of the PSs and possibly yield compounds suitable for crystallographic analysis. The coordination of monosaccharide units to transition metals, especially those of the platinum group, is well-documented.¹ Other investigations into the mechanisms of coordination, with characterization of the resulting products, have also been carried out with metals such as iron,² platinum,³ palladium,³ and copper.⁴ X-ray crystallography and spectroscopic data has shown that monosaccharides coordinate to the metal through vicinal hydroxyl or amine functional groups.

For comparison with the matrix-assisted laser desorption ionization–time of flight–mass spectrometry (MALDI-TOF-MS) spectra of putative products from reactions in which $\text{RuCl}_3 \cdot 3\text{H}_2\text{O}$ was a starting material, a MALDI-TOF-MS spectrum of $\text{RuCl}_3 \cdot 3\text{H}_2\text{O}$ was sought. The results afforded by the MALDI-TOF-MS and LDI-TOF-MS experiments carried out on $\text{RuCl}_3 \cdot 3\text{H}_2\text{O}$ are described.

Materials and methods

Mass spectrometry

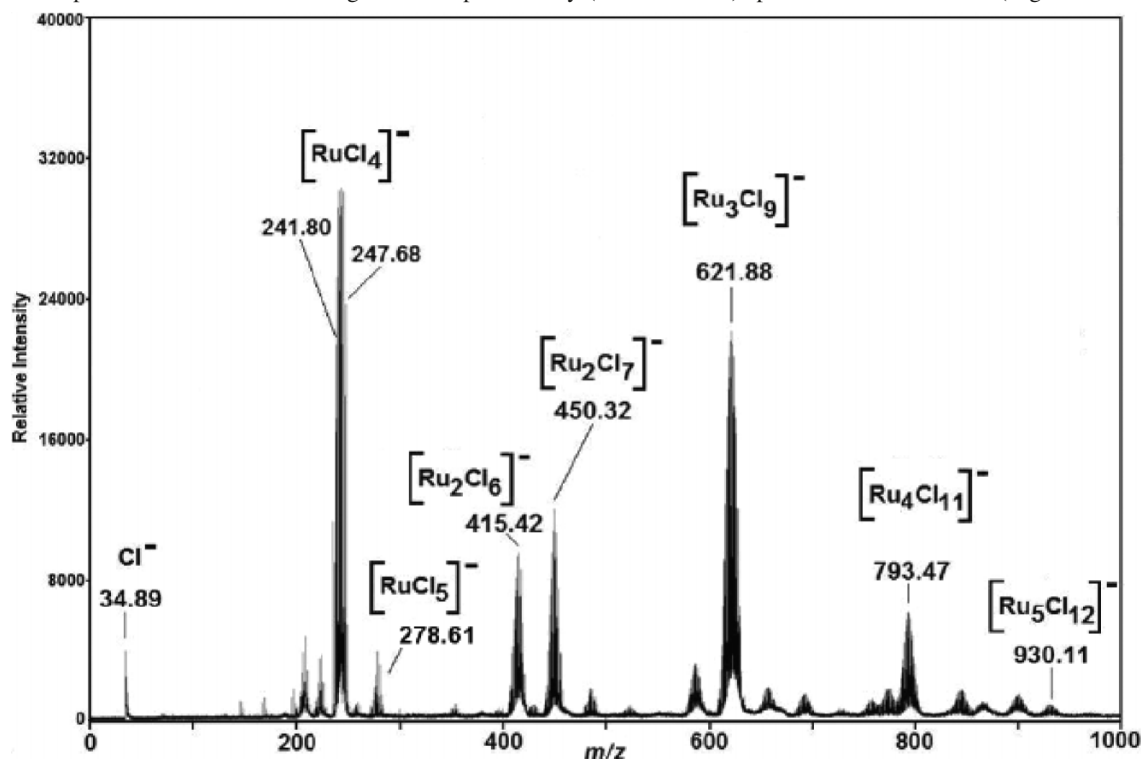
For MALDI-TOF-MS, $\text{RuCl}_3 \cdot 3\text{H}_2\text{O}$ was mixed directly with a matrix solution composed of 2 mg of 3,4-dihydroxybenzoic acid in 20% of ethanol. An analyte–matrix 1:2 ratio (v/v) and 1 μL was spotted on the MALDI sample target and allowed to dry at room temperature. For LDI-TOF-MS, a few crystals of analyte were deposited on the sample target and gently pressed toward the target. The analyses were performed using a MALDI-TOF-MS instrument (model Reflex III, Bruker) equipped with a 337 nm nitrogen laser. Samples were analyzed in reflectron and negative ion modes. Ion sources 1 and 2 were held at 20 and 16.35 kV, respectively. The guiding lens voltage was set at 9.75 kV. The reflector detection gain was set at 5.3 with pulsed ion extraction at 200 ns. The nitrogen laser power was set to the minimum level necessary to generate a reasonable signal and avoid possible degradation of analytes. Typically, 15% of laser energy was used, which was calculated to be 4 mJ. In the case of high laser energy experiments, 45% of laser energy was used, which equalled 12.5 mJ. The pulse duration was 9 Hz, the spot size was 2 mm, and the calculated energy density was 100 $\mu\text{J}/0.1 \text{ mm}^2$. A two-point external calibration was

Received 16 September 2010. Accepted 1 December 2010. Published on the NRC Research Press Web site at canjchem.nrc.ca on 24 March 2011.

A.G. Boncheff and M.A. Monteiro.¹ Department of Chemistry, University of Guelph, Guelph, ON N1G 2W1, Canada.

¹Corresponding author (e-mail: monteiro@uoguelph.ca).

Fig. 1. Laser desorption ionization–time of flight–mass spectrometry (LDI-TOF-MS) spectrum of $\text{RuCl}_3 \cdot 3\text{H}_2\text{O}$ (negative mode).



performed, using the $[\text{M} - \text{H}]^{-1}$ (153.01 Da) and $[2\text{M} - \text{H}]^{-2}$ (447.12 Da) peaks of dehydroxybenzoic acid and the dimer of sinapinic acid, respectively, prepared in acetonitrile–water solution (10 pmol/ μL). Ruthenium(III) trichloride trihydrate was purchased from Pressure Chemicals (Pittsburgh, Pennsylvania).

Computations

All geometry optimization and vibrational frequency analysis density functional theory (DFT) calculations were performed using Gaussian09.⁵ All calculations used the PBE0 exchange–correlation functional⁶ with a dual basis set; SDD⁷ was used for the Ru atoms and 6–311G(2d) was used for the Cl atoms. The composition of molecular orbitals and overlap population analysis, to determine bond orders and bonding of all species, were calculated using AOMix.^{8,9}

Results and discussion

Our first attempt, using a matrix solution of 3,4-dihydroxybenzoic acid in 20% of ethanol, yielded no easily understood m/z ions, and no ions representative of the molecular weight of $\text{RuCl}_3 \cdot 3\text{H}_2\text{O}$ or related species were observed. Subsequently, we attempted the same experiment with no matrix (LDI-TOF-MS). The LDI-TOF-MS experiment in the negative mode also showed no m/z ions attributable to $\text{RuCl}_3 \cdot 3\text{H}_2\text{O}$ or associated residues, but afforded a series of low and high m/z ions of defined compositions with an isotope pattern that suggested the presence of ruthenium- and chloride-containing species (Fig. 1).

The most intense m/z ion at 243.69 was attributed to a complex containing one Ru atom and four Cl atoms, $[\text{RuCl}_4]^{-}$. Dominant species containing two Ru atoms were

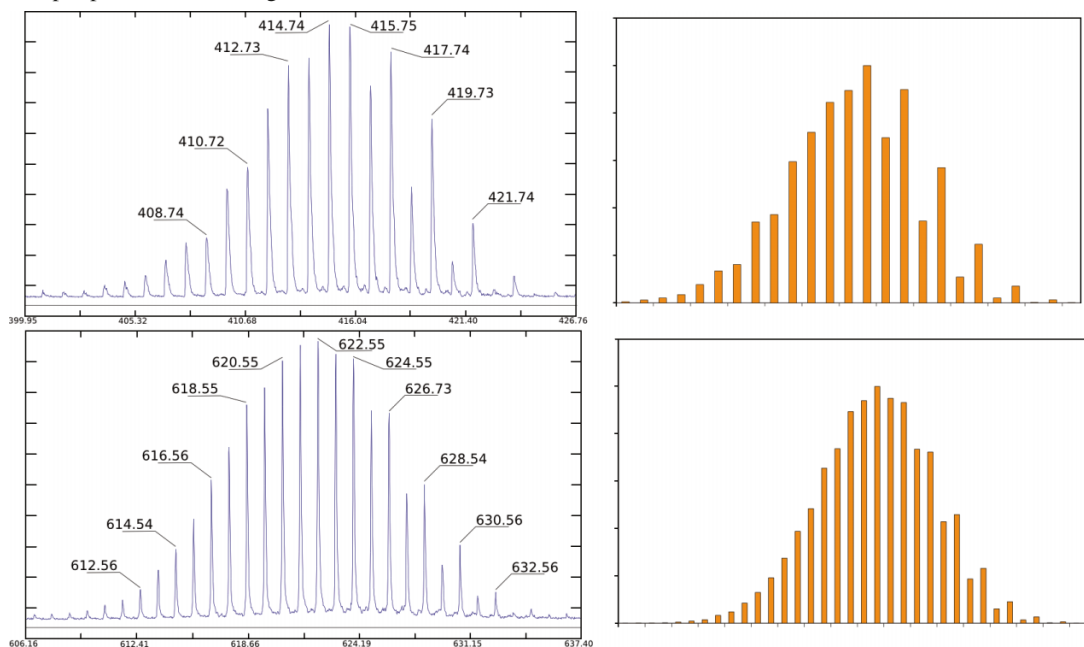
observed at m/z 415.42 for $[\text{Ru}_2\text{Cl}_6]^{-}$ and at m/z 450.32 for $[\text{Ru}_2\text{Cl}_7]^{-}$. Two other intense ions containing three and four Ru atoms were observed at m/z 621.88 for $[\text{Ru}_3\text{Cl}_9]^{-}$ and at 793.47 for $[\text{Ru}_4\text{Cl}_{11}]^{-}$. Although of low intensity, m/z ions attributable to $[\text{RuCl}_5]^{-}$ and $[\text{Ru}_5\text{Cl}_{12}]^{-}$ complexes were also observed at m/z 278.61 and 930.11, respectively. Computer-generated isotopic distribution profiles for the described compositions matched the observed experimental data (Fig. 2). However, that of $[\text{RuCl}_4]^{-}$ suggested that this m/z peak could also contain $[\text{RuCl}_3 \cdot 2\text{OH}]^{-}$. Within the limits of detection, no other higher mass ions were observed.

Based on computational studies, a structure is proposed for each cluster, and, in particular, we suggest cyclic conformations for the larger complexes, $[\text{Ru}_3\text{Cl}_9]^{-}$, $[\text{Ru}_4\text{Cl}_{11}]^{-}$, and $[\text{Ru}_5\text{Cl}_{12}]^{-}$. Figure 3 shows the proposed cluster structures with their respective total energy values. DFT calculations showed that the proposed noncyclic structures of $[\text{RuCl}_4]^{-}$ and $[\text{Ru}_2\text{Cl}_6]^{-}$ favoured a planar and tetrahedral-like geometry, respectively (Fig. 3). As $[\text{RuCl}_4]^{-}$ and $[\text{Ru}_2\text{Cl}_6]^{-}$ are both doublet species, an unrestricted PBE0 method was used for the calculations, with the S^2 values for $[\text{RuCl}_4]^{-}$ and $[\text{Ru}_2\text{Cl}_6]^{-}$ being 0.7503 and 0.7547, respectively, after annihilation of the first-order spin contaminant. A square pyramidal geometry was attributed to the $[\text{RuCl}_5]^{-}$, a closed shell singlet species with an S^2 value of 0.0000.

The proposed $[\text{Ru}_2\text{Cl}_7]^{-}$ cluster contains two Ru atoms bonded together with a single bond and three chloride bridges (Fig. 3). Two terminal chlorides extended from each Ru atom. As a singlet species, the $[\text{Ru}_2\text{Cl}_7]^{-}$ cluster optimization had an S^2 value of 0.0000.

For the $[\text{Ru}_3\text{Cl}_9]^{-}$ complex, one of the most intense m/z ions, the structure is composed of a series of three-membered

Fig. 2. Mass spectral profile of the isotopic pattern of $[\text{Ru}_2\text{Cl}_6]^-$ (top) and $[\text{Ru}_3\text{Cl}_9]^-$ (bottom). The experimental spectrum is at the left and the computed isotopic pattern is at the right.



rings lying on a single plane (Fig. 3). The proposed structure of the $[\text{Ru}_3\text{Cl}_9]^-$ cluster bares a strong resemblance to the DFT geometry optimizations of $[\text{Re}_3(\mu\text{-Cl})_3\text{Cl}_9]^{-3}$ described by Psaroudakis et al.¹⁰ Both molecules contain a three-membered ring of metal atoms with each metal atom being connected to two in-plane bridging chlorides and two out-of-plane terminal chlorides. The optimization of the $[\text{Ru}_3\text{Cl}_9]^-$ cluster gave an S^2 value of 0.0000 (singlet species).

For the $[\text{Ru}_4\text{Cl}_{11}]^-$ cluster, we first envisaged a bicyclo[3.3.1]nonane-like structure; however, a molecular orbital overlap population analysis to determine bonding suggested the cyclic structure presented in (Fig. 3). As a singlet species, the $[\text{Ru}_4\text{Cl}_{11}]^-$ cluster optimization had an S^2 value of 0.0000. For $[\text{Ru}_5\text{Cl}_{12}]^-$, we hypothesized a tetracyclic[3.3.3.1.1]tridecane-like structure, in which all Ru atoms were connected to each other through Cl bridges. However, the computational calculations afforded the structure shown in Fig. 3. To obtain convergence, the optimization and frequency calculations on the $[\text{Ru}_5\text{Cl}_{12}]^-$ cluster were performed with loose convergence criteria (1×10^{-6}) for the self-consistent field (SCF) energy. The optimization showed that $[\text{Ru}_5\text{Cl}_{12}]^-$ is a highly symmetric molecule with Ru atoms in both planar and tetrahedral configurations. An S^2 value of 0.9106 resulted for this unrestricted calculation and one virtual frequency was reported from the vibrational analysis. Geometry optimization and vibrational analysis of the neutral $[\text{Ru}_5\text{Cl}_{12}]$ cluster was also performed and was successful under the default convergence criteria with no virtual frequencies reported. A comparison between the optimized neutral $[\text{Ru}_5\text{Cl}_{12}]$ and anionic $[\text{Ru}_5\text{Cl}_{12}]^-$ clusters showed they were visually similar. The observed difficulties in the convergence of the anionic $[\text{Ru}_5\text{Cl}_{12}]^-$ cluster under default criteria is thought to arise from the highly delocalized HOMO, which contains the unpaired electron for this doublet species. Except for $[\text{Ru}_5\text{Cl}_{12}]^-$, no imaginary frequencies were reported for the optimized geometries, indi-

cating that an energy minimum was reached for the aforementioned cases.

We suggest that the cyclic $[\text{Ru}_3\text{Cl}_9]^-$, $[\text{Ru}_4\text{Cl}_{11}]^-$ and $[\text{Ru}_5\text{Cl}_{12}]^-$ clusters may be in part formed through intranucleophilic substitutions in the gas phase, and, to some extent, the presence of m/z 35 $[\text{Cl}]^-$ in the LDI-TOF-MS spectrum (Fig. 1) lends support to this hypothesis. In addition to the structures shown in Fig. 3, other structural arrangements for $[\text{Ru}_2\text{Cl}_7]^-$, $[\text{Ru}_3\text{Cl}_9]^-$, and $[\text{Ru}_4\text{Cl}_{11}]^-$ were also observed to minimize, but at higher total energies (Fig. 4).

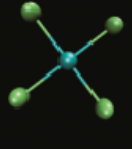
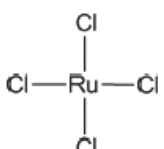
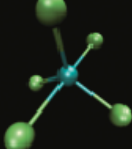
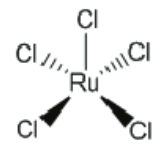
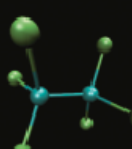
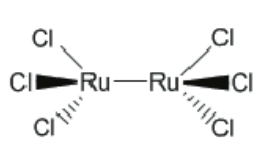
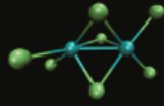
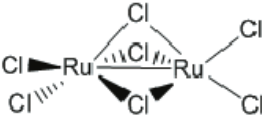
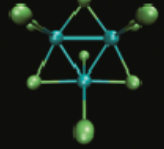
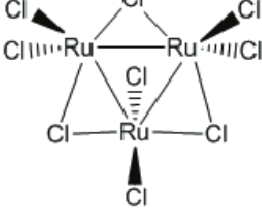
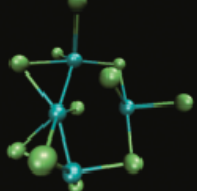
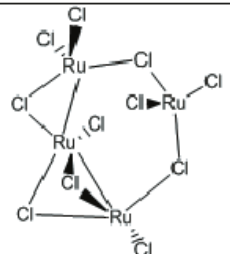
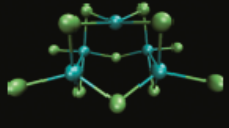

As mentioned, we suggested that the m/z ions at 622.30 and 794.30 corresponded to cyclic clusters of $[\text{Ru}_3\text{Cl}_9]^-$ and $[\text{Ru}_4\text{Cl}_{11}]^-$, respectively; but, the possibility exists that these m/z ions could be adduct compounds in the form of $[\text{Ru}_3\text{Cl}_8 + \text{Cl}]^-$ and $[\text{Ru}_4\text{Cl}_{10} + \text{Cl}]^-$. Similarly, $[\text{RuCl}_5]^-$ could exist in the form of a $[\text{RuCl}_4 + \text{Cl}]^-$ adduct. However, neutral clusters of $[\text{RuCl}_4]$, $[\text{Ru}_3\text{Cl}_8]$, and $[\text{Ru}_4\text{Cl}_{10}]$ were not converged in the SCF during optimization. Thus, we suggest that there is a low probability that these adductlike clusters exist. In the proposed structures (Figs. 3 and 4), there were no data that would suggest the presence of double or triple bonds between the Ru atoms.

Neighbouring the high-intensity m/z ions, ions of much lower intensity could be observed that differed by m/z 35. These could be generated by loss of Cl atoms from the described clusters or could represent other species. Although of very low intensity, other ions at m/z 208.77, 224.72, 278.64, 844.12, and 874.51 might be attributed to $[\text{RuCl}_3]^-$, $[\text{RuCl}_3\text{:OH}]^-$, $[\text{RuCl}_4\text{:2OH}]^-$, $[\text{Ru}_4\text{Cl}_{10}\text{:OH}]^-$, and $[\text{Ru}_5\text{Cl}_9\text{:2OH}]^-$, respectively.

Conclusions

We have shown that gas-phase Ru_xCl_y clusters may be synthesized by the laser ablation of $\text{RuCl}_3 \cdot 3\text{H}_2\text{O}$ in the

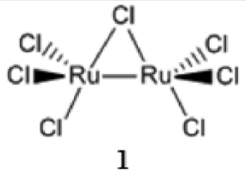
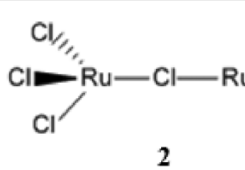
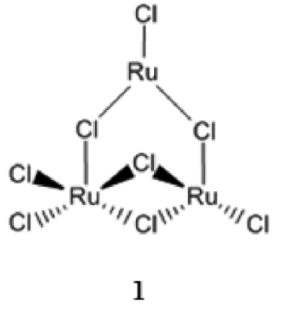
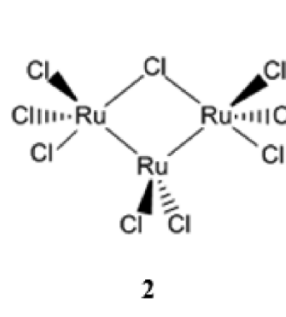
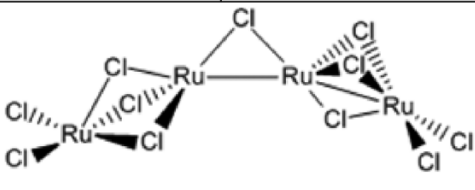
Fig. 3. Optimized ruthenium chloride cluster structures.

Formula and Total Energy (kJ/mol)	Cluster Model	Cluster Structure
[RuCl₄]⁻ $E = -5.0811 \times 10^6$		
[RuCl₅]⁻ $E = -6.2892 \times 10^6$		
[Ru₂Cl₆]⁻ $E = -7.7464 \times 10^6$		
[Ru₂Cl₇]⁻ $E = -8.9543 \times 10^6$		
[Ru₃Cl₉]⁻ $E = -1.1612 \times 10^7$		
[Ru₄Cl₁₁]⁻ $E = -1.4285 \times 10^7$		
[Ru₅Cl₁₂]⁻ $E = -1.5742 \times 10^7$		

negative ion mode. Based on computational calculations, Figs. 3 and 4 show proposed structures for the ruthenium chloride clusters. However, other structural isomers may be possible. Cluster formation was found to be inhibited when 3,4-dihydroxybenzoic acid was used as the matrix. The MS

data showed that the Ru–Cl ratio decreases as the number of Ru atoms increase and that the higher order clusters contain a mixed oxidation state. Other examples of cluster formations by LDI containing various transition metals have been described.^{11–13} Also, a wide range of metal clusters have

Fig. 4. Optimized ruthenium chloride cluster structures with higher total energies.

Formula and Total Energy (kJ/mol)	Cluster Structure	
$[\text{Ru}_2\text{Cl}_7]^-$ 1. $E = -8.954323 \times 10^6$ 2. $E = -8.954208 \times 10^6$	 1	 2
$[\text{Ru}_3\text{Cl}_9]^-$ 1. $E = -1.161929 \times 10^7$ 2. $E = -1.161946 \times 10^7$	 1	 2
$[\text{Ru}_4\text{Cl}_{11}]^-$ $E = -1.4284 \times 10^7$		

been produced by LDI of metal oxides, metal phosphides, metal chalcogenides, and metal carbonyls.¹¹ Similarly to the results obtained here, it has been reported that the use of a matrix prevented the formation of these types of metal-containing clusters.^{11,12} Large rhenium chloride clusters have also been observed to be generated by LDI of rhenium trichloride,¹² with cluster formation only being afforded under negative mode ionization.¹²

Although reports describing the production of gas-phase transition-metal clusters are typically limited to laser ablation methods, work by Wang and Wang¹⁴ showed that electrospray ionization (ESI) of alkali and alkali-earth metal halide solutions lead to the generation of various metal cluster dianions. However, they were unable to observe cluster formation from metal halide solutions of any of the 3d transition-metal elements. Although gas-phase clusters may not have a solution or solid-state counterpart, O'Hair and Khairallah¹³ produced gas-phase metal clusters in a MALDI-TOF-MS apparatus that could be employed as catalysts, and thus the ruthenium chloride clusters described in this work could prove to be useful chemical compounds.

Acknowledgement

This work was funded by Natural Sciences and Engineering Research Council of Canada (NSERC).

References

- (1) Allscher, T.; Klüfers, P.; Mayer, P. *Glycoscience* **2008** (4): 1077. doi:10.1007/978-3-540-30429-6_24.
- (2) Geetha, K.; Raghavan, M. S. S.; Kulshreshtha, S. K.; Sasikala, R.; Rao, C. P. *Carbohydr. Res.* **1995** 271 (2), 163. doi:10.1016/0008-6215(95)00050-4.
- (3) Schwarz, T.; Heß, D.; Klüfers, P. *Dalton Trans.* **2010** 39 (23), 5544. doi:10.1039/c002711a.
- (4) Striegler, S.; Dittel, M. *Inorg. Chem.* **2005** 44 (8), 2728. doi:10.1021/ic048724p.
- (5) Frisch, M. J.; Trucks, G. W.; Schlegel, H. B.; Scuseria, G. E.; Robb, M. A.; Cheeseman, J. R.; Scalmani, G.; Barone, V.; Mennucci, B.; Petersson, G. A.; Nakatsuji, H.; Caricato, M.; Li, X.; Hratchian, H. P.; Izmaylov, A. F.; Bloino, J.; Zheng, G.; Sonnenberg, J. L.; Hada, M.; Ehara, M.; Toyota, K.; Fukuda, R.; Hasegawa, J.; Ishida, M.; Nakajima, T.; Honda, Y.; Kitao, O.; Nakai, H.; Vreven, T.; Montgomery, J. A., Jr.; Peralta, J. E.; Ogliaro, F.; Bearpark, M.; Heyd, J. J.; Brothers, E.; Kudin, K. N.; Staroverov, V. N.; Kobayashi, R.; Normand, J.; Raghavachari, K.; Rendell, A.; Burant, J. C.; Iyengar, S. S.; Tomasi, J.; Cossi, M.; Rega, N.; Millam, J. M.; Klene, M.; Knox, J. E.; Cross, J. B.; Bakken, V.; Adamo, C.; Jaramillo, J.; Gomperts, R.; Stratmann, R. E.; Yazyev, O.; Austin, A. J.; Cammi, R.; Pomelli, C.; Ochterski, J. W.; Martin, R. L.; Morokuma, K.; Zakrzewski, V. G.; Voth, G. A.; Salvador, P.; Dannenberg, J. J.; Dapprich, S.; Daniels, A. D.; Farkas, O.; Foresman, J. B.; Ortiz, J. V.; Cioslowski, J.; Fox, D. J. *Gaussian 09*, Revision A.02; Gaussian, Inc.: Wallingford, CT, 2009.
- (6) Adamo, C.; Barone, V. *J. Chem. Phys.* **1999** 110 (13), 6158. doi:10.1063/1.478522.
- (7) Andrae, D.; Häyßermann, U.; Dolg, M.; Stoll, H.; Preuß, H. *Theor. Chem. Acc.* **1990** 77 (2), 123. doi:10.1007/BF01114537.

- (8) Gorelsky, S. I. *AOMix: Program for Molecular Orbital Analysis*, version 6.4; University of Ottawa; Ottawa, ON, 2010. <http://www.sg-chem.net>.
- (9) Gorelsky, S. I.; Lever, A. B. P. *J. Organomet. Chem.* **2001** 635 (1–2), 187. doi:10.1016/S0022-328X(01)01079-8.
- (10) Psaroudakis, N.; Mertis, K.; Liakos, D. G.; Simandiras, E. D. *Chem. Phys. Lett.* **2003** 369 (3–4), 490. doi:10.1016/S0009-2614(02)02045-6.
- (11) McIndoe, J. S. *Trans. Met. Chem. (Weinh.)* **2003** 28 (1), 122. doi:10.1023/A:1022515104991.
- (12) Dopke, N. C.; Treichel, P. M.; Vestling, M. M. *Inorg. Chem.* **1998** 37 (6), 1272. doi:10.1021/ic971220p.
- (13) O'Hair, R. A. J.; Khairallah, G. N. *J. Cluster Sci.* **2004** 15 (3), 331. doi:10.1023/B:JOCL.0000041199.40945.e3.
- (14) Wang, X. B.; Wang, L. S. *Phys. Rev. Lett.* **1999** 83 (17), 3402. doi:10.1103/PhysRevLett.83.3402.